Articles

Supramolecular Coordination Chemistry in Aqueous Solution: Lanthanide Ion-Induced Triple Helix Formation

Jeremy J. Lessmann and William DeW. Horrocks, Jr.*

Department of Chemistry, The Pennsylvania State University, University Park, Pennsylvania, 16802

Received June 15, 1999

The self-assembly of dinuclear triple helical lanthanide ion complexes (helicates), in aqueous solution, is investigated utilizing laser-induced, lanthanide luminescence spectroscopy. A series of dinuclear lanthanide(III) helicates (Ln(III)) based on 2,6-pyridinedicarboxylic acid (dipicolinic acid, dpa) coordinating units was synthesized by linking two dpa moieties using the organic diamines (1*R*,2*R*)-diaminocyclohexane (chxn-*R*,*R*) and 4,4′-diaminodiphenylmethane (dpm). Luminescence excitation spectroscopy of the Eu^{3+} $^7F_0 \rightarrow {}^5D_0$ transition shows the apparent cooperative formation of neutral triple helical complexes in aqueous solution, with a $[Eu_2L_3]$ stoichiometry. Eu^{3+} excitation peak wavelengths and excited-state lifetimes correspond to those of the $[Eu(dpa)_3]^{3-}$ model complex. CD studies of the Nd(III) helicate Nd_2(dpa-chxn-*R*,*R*)$_3$ reveal optical activity of the f−f transitions, indicating that the chiral linking group induces a stable chirality at the metal ion center. Molecular mechanics calculations using CHARMm suggest that the ΔΔ configuration at the Nd^{3+} ion centers is induced by the chxn-*R*,*R* linker. Stability constants were determined for both ligands with Eu^{3+}, yielding identical results: $\log K = 31.6 \pm 0.2$ (K in units of M^{-4}). Metal−metal distances calculated from $Eu^{3+} \rightarrow Nd^{3+}$ energy-transfer experiments show that the complexes have metal−metal distances close to those calculated by molecular modeling. The fine structure in the Tb^{3+} emission bands is consistent with the approximate D_3 symmetry as anticipated for helicates.

Introduction

Supramolecular chemistry refers to the spontaneous self-assembly of molecular architectures from smaller components. Examples include monolayer assembly, membrane formation, molecular recognition (i.e., substrate binding to proteins, DNA/protein interactions, antibody/antigen interactions), and metal ion coordination.[1−7] All of these topics involve either the formation of discrete oligomeric species from the intermolecular association of a few components (receptor/substrate interactions, metal ion binding) or the formation of polymolecular species from the spontaneous association of a large number of components into a well-defined macroscopic system (membrane or monolayer formation, micelle formation, solid-state structures).[1,2]

Such structures are held together by relatively weak intermolecular forces which include hydrogen-bonding, van der Waals interactions, hydrophobic/hydrophilic interactions, ionic forces, and relatively labile metal ion−ligand coordination interactions of a largely electrostatic nature. Metal−ligand interactions are generally quite labile, and the structures formed are the thermodynamically most stable products.

The focus of this work is the self-assembly of helicates. A helicate (the term first used by Lehn and co-workers in 1987)[8] is a polynuclear helical complex composed of either two or three ligand strands and two or more metal ions. They involve two or three acyclic ligands each having two or more metal ion binding sites. The ligands organize themselves around the metal ions, forming the classical intertwining structures of double or triple helices. Many previous studies of helicates have involved double and triple helical structures based on Cu^+, Ag^+, and Ni^{2+} with bipyridine and terpyridine-derived ligands, in nonaqueous solvents, although helicates based on catechol binding sites and other planar nitrogen heterocyclic ligands have also been studied in nonaqueous and aqueous solvents.[9−13] There are three known homodinuclear helicates involving lanthanide ions[10−13] and three heterodinuclear helicates involving both d and f element ions.[14−16]

(1) Lehn, J.-M. *Supramolecular Chemistry: Concepts and Perspectives*; VCH: Weinheim, Germany, 1995.
(2) Lehn, J.-M. *Science* **1993**, *260*, 1762−1763.
(3) Constable, E. C.; Smith, D. *Chem. Br.* **1995**, Jan, 33−37, 41.
(4) Lindsey, J. S. *New J. Chem.* **1991**, *15*, 153−180.
(5) Lawrence, D. S.; Jiang, T.; Levett, M. *Chem. Rev.* **1995**, *95*, 2229−2260.
(6) Lehn, J.-M. In *Perspectives in Coordination Chemistry*; Williams, A. F., Floriani, C., Merbach, A. E., Eds.; Verlag Helvitica Chimica Acta: Basel, 1992; pp 447−462.
(7) Sabbatini, N.; Guardigli, M.; Lehn, J.-M. *Coord. Chem. Rev.* **1993**, *123*, 201−228.
(8) Lehn, J.-M.; Rigault, A.; Siegel, J.; Harrowfield, J.; Chevrier, B.; Moras, D. *Proc. Natl. Acad. Sci. U.S.A.* **1987**, *84*, 2565.
(9) Piguet, C.; Bernardinelli, G.; Hopfgartner, G. *Chem. Rev.* **1997**, *97*, 2005−2062.
(10) Piguet, C.; Bunzli, J.-C. G.; Bernardinelli, G.; Hopfgartner, G.; Williams, A. F. *J. Am. Chem. Soc.* **1993**, *115*, 8197.
(11) Martin, N.; Bunzli, J.-C.; McKee, V.; Piguet, C.; Hopfgartner, G. *Inorg. Chem.* **1998**, *37*, 577−589.
(12) Elhabiri, M.; Scopelliti, R.; Bunzli, J.-C. G.; Piguet, C. *J. Chem. Soc., Chem. Commun.* **1998**, 2347−2348.
(13) Elhabiri, M.; Scopelliti, R.; Bünzli, J.-C. G.; Piguet, C. *J. Am. Chem. Soc.* **1999**, *121*, 10747−10762.
(14) Edder, C.; Piguet, C.; Bunzli, J.-C. G.; Hopfgartner, G. *J. Chem. Soc., Dalton Trans.* **1997**, 4657−4663.

10.1021/ic990698l CCC: $19.00 © 2000 American Chemical Society
Published on Web 06/28/2000

Heretofore, most helicates have been formed and studied in aprotic solvents, usually acetonitrile.[17−20] Characterization of these complexes has depended largely upon electrospray mass spectrometry, NMR techniques, and X-ray crystallography to establish speciation and structural information.[9,21] Optical techniques, mainly UV−vis spectroscopy, have been used to characterize and follow the formation of helicates in solution.[9,22] Luminescence studies, primarily of microcrystalline samples of certain lanthanide helicates, have also recently been reported.[10,11,14]

Interest in the self-assembly of helicates and other metal-based supramolecular structures has arisen, in a large part, due to the potential for the self-assembly of molecular devices and nanostructures. Possibilities include photonic devices, electronic devices (molecular wires, etc.), ionic devices, switches, nonlinear optical materials, and novel architectures with structural features such as grids, cylinders, and circles.[1,6,7,9,23−25] Lanthanide-based helicates have been investigated due to their potential for use as light-converting molecular devices.[7,14,15,20,26] There may also be potential uses for lanthanide-based helical structures in sensing or diagnostic applications.

In contrast to most of the previous studies on triple helicates, which have been carried out in nonaqueous solvents, the present research investigates the formation, in aqueous solution, of neutral triple helicates based on lanthanide ions. In this work we report the second example of a neutral helicate. The first[12] appeared as this work was nearing completion, followed by a full report.[13] Only three other examples of helicates formed in aqueous solution have been reported previously.[12−14,27]

The design concept of the present helicate-forming ligands, L, is the linking of two tridentate chelating units via organic diamines such that each ligand will coordinate to two different metal ions and the complexes formed will be dinuclear with two 9-coordinate lanthanide ions and a stoichiometry of $[Ln_2L_3]$. The coordinating units chosen are based on the well-known dpa ligand (dpa = 2,6-pyridinedicarboxylic acid) which forms the well-studied,[28−31] propeller-shaped, complex $[Ln(dpa)_3]^{3-}$ which is 9-coordinate with a trigonal prismatic, D_3, geometry and either Δ or Λ chirality at the metal center. The diamines link the coordinating moieties via amide bonds. The acyclic diamine dpa-dpm (dpm = 4,4′-diaminodiphenylmethane) is analogous to a fairly rigid linker successfully used in heterocyclic nitrogen ligand helicates.[10−13] The chiral linker dpa-chxn-*R,R* (*S,S*) was chosen so as to impose a handedness to the helicate as a whole and to produce a complex which retains its metal-centered ($\Delta\Delta$ or $\Lambda\Lambda$) optical activity in solution. $[Ln(dpa)_3]^{3-}$ and other chiral lanthanide complexes of this type all racemize rapidly in solution, resulting in racemic mixtures.

Laser-induced lanthanide luminescence spectroscopy in aqueous solution has been shown to be an extremely useful technique to study the formation and speciation of lanthanide chelates[32−37] and is the major technique employed in the present study. Molecular mechanical modeling calculations have guided this study and have been used to predict the likely structures of dinuclear helicates with a 3/2 ligand/metal (L/M) stoichiometry and D_3 symmetry. Metal−metal distances estimated from the models are compared to distances derived from $Eu^{3+} \rightarrow Nd^{3+}$ luminescence energy transfer measurements.[36,38]

Experimental Section

Materials. Dpm was purchased from TCI America. HEPES (J. T. Baker, free acid, ultrapure bioreagent) was purchased from VWR. D_2O was purchased from Isotec Inc. All other solvents, starting materials, and $LnCl_3$ salts were purchased from Aldrich. All chemicals were used as received. Solvents were at least HPLC grade. Silica gel (Merk, 230−400 mesh, 60 Å) was used for preparative chromatography. The water used was distilled, and deionized using a NANOpure system.

Spectroscopic Measurements. General Techniques. Circular dichroism spectra were obtained on an Aviv model 62DS circular dichroism spectrometer. ^{1}H NMR spectra were obtained on a Bruker DPX-300 spectrometer. Shifts are referenced in parts per million from TMS in $CDCl_3$ and the HOD peak (4.8 ppm) in D_2O. Terbium luminescence spectroscopy was performed on a SPEX Fluorolog-2 fluorescence spectrometer (single monochromators for both excitation and emission pathways).

Laser-Induced Luminescence. Eu^{3+} excitation spectra and excited-state lifetimes were obtained on a Continuum YG 581C pulsed (10 Hz) Nd:YAG laser pumped tunable TDL 50 dye laser. A mixture of Rhodamine 590 and 610 dyes was used to scan a region from 577 to 582 nm to access the $^7F_0 \rightarrow {}^5D_0$ transition of Eu^{3+}. The $^5D_0 \rightarrow {}^7F_2$ emission was monitored at 614 nm. The laser operates at 10 Hz, producing 50−70 mJ/pulse with this dye mixture. The dye laser has a pulse width of 7 ns with a resolution of 0.01 nm at 560 nm. Luminescence is sampled 90° to the incident laser beam, and is focused onto a 0.2 m double monochromator (Instruments SA, DH-20-V-IR) and subsequently detected by a Hammamatsu type R928 HA photomultiplier tube. The signal is collected by a LeCroy data acquisition system interfaced to a 386 processor-based personal computer.[36]

Analysis of Eu^{3+} Luminescence Data. Spectral peak fitting and lifetime analysis were achieved using the commercial program PeakFit (SPSS Inc.). This program employs a Marquardt nonlinear regression algorithm. Eu^{3+} excitation spectra were fit to a Lorentzian−Gaussian

(15) Piguet, C.; Hopfgartner, G.; Williams, A. F.; Bunzli, J.-C. *J. Chem Soc., Chem. Commun.* **1995**, 491−493.
(16) Piguet, C.; Bernardinelli, G.; Bünzli, J.-C. G.; Petoud, S.; Hopfgartner, G. *J. Chem. Soc., Chem. Commun.* **1995**, 2575.
(17) Garret, T. M.; Koert, U.; Lehn, J.-M.; Rigault, A.; Meyer, D.; Fischer, J. *J. Chem. Soc., Chem. Commun.* **1990**, 557−558.
(18) Pfeil, A.; Lehn, J.-M. *J. Chem. Soc., Chem. Commun.* **1992**, 838−840.
(19) Williams, A. F.; Piguet, C.; Bernardinelli, G. *Angew. Chem., Int. Ed. Engl.* **1991**, *30*, 1490−1492.
(20) Bernardinelli, G.; Piguet, C.; Williams, A. F. *Angew. Chem., Int. Ed. Engl.* **1992**, *31*, 1622−1624.
(21) Marquis-Rigault, A.; Dupont-Gervais, A.; Van Dorsselaer, A.; Lehn, J.-M. *Chem. Eur. J.* **1996**, *2*, 1395.
(22) Williams, A. F.; Piguet, C.; Carina, R. F. In *Transition Metals in Supramolecular Chemistry*; Fabbrizzi, L., Poggi, A., Eds.; Kluwer Academic Publishers: Amsterdam, 1994; pp 409−424.
(23) Constable, E. C. In *Transition Metals in Supramolecular Chemistry*; Fabbrizzi, L., Poggi, A., Eds.; Kluwer Academic Publishers: Amsterdam, 1994; pp 81−99.
(24) Baxter, P. N. W.; Lehn, J.-M.; Kneisel, B. O.; Fenske, D. *Angew. Chem., Int. Ed. Engl.* **1997**, *36*, 1978−1981.
(25) Hasenknopf, B.; Lehn, J.-M.; Boumediene, N.; Dupont-Gervais, A.; Van Dorsslaer, A.; Kneisel, B.; Fenske, D. *J. Am. Chem. Soc.* **1997**, *119*, 10956−10962.
(26) Piguet, C.; Williams, A. F.; Bernardinelli, G.; Bunzli, J.-C. G. *Inorg. Chem.* **1993**, *32*, 4139−4149.
(27) Enemark, E. J.; Stack, T. D. P. *Angew. Chem., Int. Ed. Engl.* **1995**, *34*, 996−998.
(28) Horrocks, W. D., Jr.; Sudnick, D. R. *Science* **1979**, *206*, 1194−1196.
(29) Trout, T. K.; Bellama, J. M.; Faltynek, R. A.; Parks, E. J.; Brinckman *Inorg, Chim. Acta* **1989**, *155*, 13.
(30) Albertsson, J. *Acta Chem. Scand.* **1972**, *26*, 1023.
(31) Desreux, J. F.; Reilley, C. N. *J. Am. Chem. Soc.* **1976**, *98*, 2105.
(32) Albin, M.; Horrocks, W. D., Jr.; Liotta, F. J. *Chem. Phys. Lett.* **1982**, *85*, 61−64.
(33) Holtz, R. C.; Chang, C. A.; Horrocks, W., DeW., Jr. *Inorg. Chem.* **1991**, *30*, 3270−3275.
(34) Holz, R. C.; Klakamp, S. L.; Chang, C. A.; Horrocks, W. D., Jr. *Inorg. Chem.* **1990**, *29*, 2651−2658.
(35) Bruno, J.; Herr, B. R.; Horrocks, W. D., Jr. *Inorg. Chem.* **1993**, *32*, 756−762.
(36) Frey, S. T.; Chang, C. A.; Carvalho, J. F.; Varadarajan, A.; Schultze, L. M.; Pounds, K. L.; Horrocks, W. D., Jr. *Inorg. Chem.* **1994**, *33*, 2882−2889.
(37) Wu, S. L.; Horrocks, W. D., Jr. *Anal. Chem.* **1996**, *68*, 394−401.
(38) Horrocks, W. D., Jr.; Sudnick, D. R. *Acc. Chem. Res.* **1981**, *14*, 384−392.

product function described elsewhere.[39] Eu^{3+} excited-state lifetimes were determined by fitting the luminescence decay spectra to a sum of exponentials.

Number of Coordinated Water Molecules. It has long been observed that the rate of decay of the Ln^{3+} excited state is directly proportional to the number of water molecules in the first coordination sphere of the lanthanide ion.[40,41] Water molecules in the first coordination sphere of the metal provide a ready nonradiative deexcitation pathway for the excited state. This is due to a weak coupling between the O−H vibrational ladder and the excited state. There is a strong isotope effect for this deexcitation process. Ln^{3+} lifetimes are longer in D_2O than in H_2O. Horrocks and Sudnick developed an equation where the number of coordinated water molecules (q) can be calculated on the basis of the OH/OD isotope effect.[41] Recently Parker and coworkers[42,43] noted that "closely diffusing" second coordination sphere solvent water molecules contribute a small amount to Eu^{3+} deexcitation. We have incorporated[44] this effect into a modification of our original equation for q,[38,41] with the parameter $\alpha = 0.30$ ms^{-1} representing the effect of second and subsequent coordination sphere molecules, and the constant A determined to be 1.11 waters·ms. The values for the constant A and α were determined from a linear least-squares fit to luminescence decay data on 25 Eu^{3+} complexes which exhibit a single $^7F_0 \rightarrow {}^5D_0$ excitation peak. This results in eq 1, where τ represents the excited-state lifetime (ms) in the solvent indicated. The standard error in q is ±0.1 water molecule.

$$q = A(\tau_{H_2O}{}^{-1} - \tau_{D_2O}{}^{-1} - \alpha) \quad (1)$$

Distance between Metal Binding Sites. Eu^{3+} can undergo a Förster-type nonradiative energy transfer if it is placed in proximity to another ion which has an absorption spectrum which overlaps with the Eu^{3+} emission spectrum.[38] From the efficiency of the energy transfer it is possible to measure the distance, r, between the two Ln^{3+} ions if no other energy-transfer process takes place. Nd^{3+} has a best overlap of any of the lanthanides with the Eu^{3+} emission, and has been used frequently as an acceptor in this type of measurement for many years.[36,45−51] The efficiency of energy transfer, E, is related to the lifetime of Eu^{3+} in both the presence, τ, and the absence, τ_0, of the energy acceptor.

$$E = 1 - (\tau/\tau_0) \quad (2)$$

The distance, r, is given by

$$r = R_0[(1 - E)/E]^{1/6} \quad (3)$$

R_0 is the critical distance for 50% energy transfer, given by

$$R_0 = (8.75 \times 10^{-25})\kappa^2\phi\eta^{-4}J \quad (4)$$

where κ^2 is the dipole−dipole orientation factor (2/3 for metal ions), ϕ is the quantum yield of the energy donor in the absence of the acceptor (estimated from τ_{H_2O}/τ_{D_2O} for Eu^{3+}), η is the index of refraction of the intervening media, and J is the spectral overlap integral

$$J = \int \epsilon(\nu)\, F(\nu)\, \nu^{-4}\, d\nu / \int F(\nu)\, d\nu \quad (5)$$

where $\epsilon(\nu)$ is the molar absorptivity of the acceptor ion and $F(\nu)$ is the luminescence emission intensity of the donor ion at frequency ν (cm^{-1}). The error in the distance calculation is on the order of ±0.8 Å. This arises from uncertainties in (a) the luminescence decay rates (about a 10% error) and (b) ϕ and J (about 12% error).

Preparation of Ligands. The synthesis of all ligands followed the general procedure as outlined in Scheme 1. This procedure is similar to one utilized by Bünzli et al.[11] for the synthesis of one of their helicate-forming ligands. 2,6-Pyridinedicarboxylic acid monobenzyl ester (dpame, pyridine-2-carboxylic acid 6-benzyl ester) was prepared according to literature procedures.[52] Dpame was refluxed in 50 mL of dichloromethane for 2 h with a 10-fold molar excess of thionyl chloride and 100 μL of DMF. The solvents were evaporated under a vacuum and pumped for at least 2 h. The resulting yellow dpame−monoacid chloride (200 mg, 1 equiv) was dissolved in dichloromethane (20 mL) and added dropwise at 0 °C to 50 mL of a stirred dichloromethane solution containing 0.5 equiv of the appropriate diamine and 1.2 equiv of triethylamine. The resulting solution was allowed to return to room temperature with stirring overnight. The solvent was evaporated off, and the brown residue was purified by column chromatography using silica gel (CH_2Cl_2/MeOH, 99/1 → 95/5). ^{1}H NMR was used to test for purity (shifts are listed below with the individual ligands) before removal of the protecting groups. After evaporation of the chromatography solvents, the ligand diester was taken up in methanol (about 20 mL), and 20 wt % Pd (10%) on activated carbon was added to the solution. The resulting mixture was stirred under hydrogen overnight. The solution was then filtered to remove the Pd catalyst. After evaporation of the MeOH, the resulting solid was taken up in 20 mL of saturated aqueous sodium carbonate. The free acid of the ligand was purified by lowering the pH of the solution to 2 using 2 M HCl and filtering off the resulting solid. A small portion of the free acid was taken up in saturated sodium carbonate in D_2O for ^{1}H NMR measurements.

***N,N′*-[(1*R*,2*R*)-Cyclohexylene)]bis(6-(carboxy)pyridine-2-carboxamide) (dpa-chxn-*R*,*R*) or the (*S*,*S*)** enantiomer was prepared by the above method, giving a pale yellow solid. ^{1}H NMR of the diester precursor in $CDCl_3$: δ 1.5−2.3 (8H, m), 4.1 (2H, s), 5.5 (4H, s), 7.4 (10H, m, Ph), 7.8 (2H, t), 8.15 (4H, m), 8.5 (2H, br d, NH). ^{1}H NMR of the ligand disodium salt in D_2O: δ 1.5−2.3 (8H, m), 4.1 (2H, s), 4.8 (HOD), 7.9 (6H, m). FAB-MS: m/z 413.4 (M + H$^+$), expected 413.

***N,N′*-[Methylenebis(phen-1,4-ylene)]bis(6-(carboxy)pyridine-2-carboxamide) (dpa-dpm)** was prepared by the above method, yielding a white solid. ^{1}H NMR of the diester precursor in $CDCl_3$: δ 4.5 (2H, s), 5.5 (4H, s), 7.4−7.7 (8H, m, Ph), 8.1(6H, m). ^{1}H NMR of the ligand disodium salt in D_2O: δ 3.5 (2H, s), 4.8 (HOD), 6.8−7.6 (8H, m), 8.1 (6H, m).

***N*-[Methyl](6-(carboxy)pyridine-2-carboxamide) (Dpa-mma).** This ligand was synthesized in a manner similar to that of the above two ligands, except that 1 equiv of the dpame−monoacid chloride was reacted with 1 equiv of methylamine (2 M solution in methanol) and 1.2 equiv of triethylamine. The synthesis resulted in a white solid. ^{1}H NMR of the ester precursor in $CDCl_3$: δ 2.9 (2H, s), 5.5 (2H, s), 7.4−7.7 (4H, m, Ph), 8.1 (3H, m) ^{1}H NMR of the ligand sodium salt in D_2O: δ 3.0 (2H, s), 4.8 (HOD), 8.1 (3H, m). ESI-MS: m/z 203.0 (M + H$^+$), expected 203.

(39) McNemar, C. W.; Horrocks, W. D., Jr. *Appl. Spectrosc.* **1989**, *43*, 816−821.
(40) Bünzli, J.-C. G.; Choppin, G. R. *Lanthanide Probes in Life, Chemical and Earth Sciences*; Elsevier Science Publishers: New York, 1989.
(41) Horrocks, W. D., Jr.; Sudnick, D. R. *J. Am. Chem. Soc.* **1979**, *101*, 334−340.
(42) Dickins, R. S.; Parker, D.; de Sousa, A. S.; Williams, J. A. G. *Chem. Commun.* **1996**, 697−698.
(43) Beeby, A.; Clarkson, I. M.; Dickins, R. S.; Faulkner, S.; Parker, D.; Royle, L.; de Sousa, A. S.; Williams, J. A. G.; Woods, M. *J. Chem. Soc., Perkin Trans.* **1999**, 493−503.
(44) Supkowski, R. M.; Horrocks, W. D., Jr. *Inorg. Chem.* **1999**, *38*, 5616−5619.
(45) Horrocks, W. D., Jr.; Rhee, M.-J.; Snyder, A. P.; Sudnick, D. R. *J. Am. Chem. Soc.* **1980**, *102*, 3650−3652.
(46) Rhee, M.-J.; Sudnick, D. R.; Arkle, V. K.; Horrocks, W. D., Jr. *Biochemistry* **1981**, *20*, 3328−3334.
(47) Snyder, A. P.; Sudnick, D. R.; Arkle, V. K.; Horrocks, W. D., Jr. *Biochemistry* **1981**, *20*, 3334−3339.
(48) Mulqueen, P.; Tingey, J. M.; Horrocks, W. D., Jr. *Biochemistry* **1985**, *24*, 6639−6645.
(49) Horrocks, W. D., Jr.; Tingey, J. M. *Biochemistry* **1988**, *27*, 413−419.
(50) Bruno, J.; Horrocks, W. D., Jr.; Beckingham, K. *Biophys. Chem.* **1996**, *63*, 1−16.
(51) Chaudhuri, D.; Amburgey, J. C.; Weber, D. J.; Horrocks, W. D., Jr. *Biochemistry* **1997**, *36*, 9674−9680.
(52) Reddy, K. V.; Jin, S.-J.; Arora, P. K.; Sfeir, D. S.; Maloney, S. C. F.; Urbach, F. L.; Sayre, L. M. *J. Am. Chem. Soc.* **1990**, *112*, 2332−2340.

Scheme 1. Synthesis Scheme for Ligands[a]

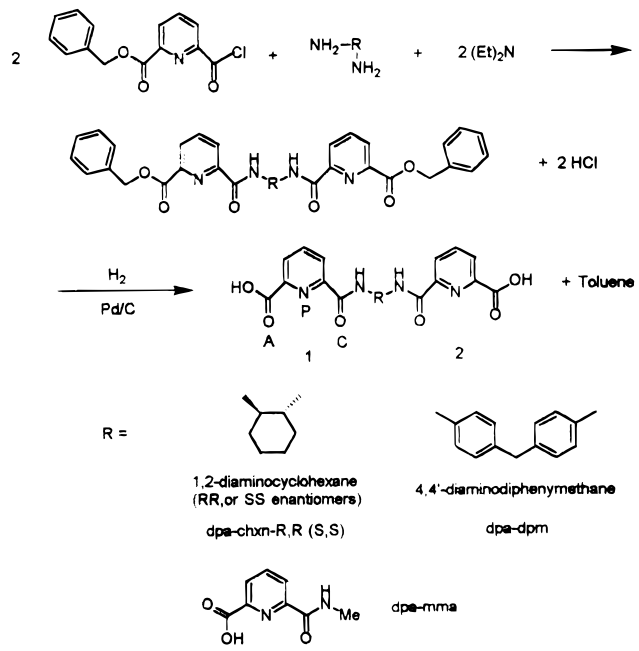

[a] Also shown are the identification labels for ligand atoms in the binding sites (for interpretation of molecular modeling) and the naming convention used for the ligands based on linker groups.

Characterization of Complexes in Solution. Determination of the Number of Isomers, Metal−Ligand Stoichiometry, and Number of Coordinated Water Molecules. Aqueous stock solutions of the ligands were prepared by weighing out the dry free acid of the ligand and adding water to make a 5 mL solution of 5−10 μM concentration. A small amount of solid sodium carbonate was added to assist in the dissolution of the free acid. The resulting solution was adjusted to about pH 7 using dilute HCl. Aqueous stock solutions of the various lanthanides were prepared by weighing out solid samples of $LnCl_3 \cdot 6H_2O$ and standardizing the resulting solution via an EDTA complexation titration using an arsenazo I as the indicator.[53]

Aqueous solutions for luminescence and absorption experiments were made by adding appropriate quantities of the ligand stock solution to 3 mL of Eu^{3+} (in the desired concentration, generally 40 μM in metal ion) in 50 mM HEPES buffer at pH 7. In most cases separate solutions were made for each point in a titration of ligand into metal. Samples were left to equilibrate overnight at 40 °C. Luminescence excitation spectra were recorded from 578 to 581.5 nm, at 21 °C. Excited-state lifetimes were taken at the excitation peak maxima.

Sensitized Tb^{3+} Emission Determination of Metal−Ligand Stoichiometry. For titrations utilizing sensitized Tb^{3+} emission, Tb^{3+} is added to 3 mL of 60 μM ligand at 25 °C under constant stirring. Tb^{3+} was added in 5 μM increments (5 μL aliquots of 6 mM stock solutions of Tb^{3+}). After each addition of metal ion the resulting solution was allowed to equilibrate for 20 min. The excitation wavelength was at 350 nm for dpa-dpm and 285 nm for dpa-chxn. At each point the intensity of the Tb^{3+} 543 nm emission band was collected for 5 min.

Inter-Metal-Ion Distances. Solutions for $Eu^{3+} \rightarrow Nd^{3+}$ energy-transfer studies of the complexes were made by adding various ratios of stock Eu^{3+} and Nd^{3+} solutions to 3 mL of ligand of the appropriate concentration (in 50 mM HEPES at pH 7 in H_2O or 50 mM HEPES at pD 7.4 in D_2O). Typical experiments utilized a 19/1 Nd^{3+}/Eu^{3+} ratio. At this ratio and at these concentrations the signal from the small amount of Eu^{3+}/Eu^{3+} complex formed is undetectable. Excited-state lifetimes were recorded at the peak maximum for each sample.

Samples for Circular Dichroism. CD of the free ligand was taken on 3 mL samples of 30 μM dpa-chxn-*R,R* (and *S,S*) in unbuffered H_2O. Concentrated (1 mL of >1 mM) solutions of complexes were made by mixing the appropriate ratio of aqueous ligand and metal stock solutions in 3 mL of DMSO followed by stirring overnight. The solutions were then lyophilized, and the resulting powders were taken up in 1 mL of DMSO.

Table 1. Parameters Used in Molecular Modeling Calculations

atom	CHARMm type	partial charge	r_{min}	e_{min}
Eu^{3+}	MEU	+3.00	1.800	−0.2000
amine N	NT	−0.40	1.650	−0.1500
amide carbonyl O	O	−0.55	1.550	−0.1591
pyridine N	N6R	−0.54	1.830	−0.0900
carboxylate charged O	OT	−0.65	1.550	−0.1591
carboxylate carbonyl O	OAC	−0.55	1.520	−0.1591

Luminescence Experiments in Acetonitrile. Solutions for luminescence experiments of dpa-chxn-*R,R* in CH_3CN were prepared by a method similar to that used by Bünzli et al.[11] for their helicates. Nonaqueous stock solutions of the ligands were prepared by adding dry free acid to about 5 mL of $CHCl_3$. A stock solution of $Eu(CF_3SO_3)_3$ (Eu-triflate) in acetonitrile was prepared by the same method used for aqueous solutions; 5 mL of 15.4 mM dpa-chxn-*R,R* in $CHCl_3$ was added dropwise, with stirring, to 5 mL of 10.3 mM Eu-triflate in acetonitrile. The mixture was allowed to stir at room temperature for 1 h. The solvent was then evaporated, and the resulting white residue was used for spectroscopic studies.

Molecular Mechanics Calculations. Modeling calculations were carried out on an IBM RISC 6000 graphics workstation running QUANTA (version 4.1.1) and CHARMm (version 2.3.1) (Molecular Simulations Inc.) molecular mechanics/dynamics software. In these calculations lanthanide ions are treated as nonbonded entities, wherein the metal ions are bound to ligands by Coulomb forces only. In this approach the equilibrium metal−ligand bond distances are determined by the balance between the Coulomb attraction of the negative partial charges on the ligand atoms and the positive charge on the metal ion and the van der Waals repulsion between the metal and ligand atoms.[36] Table 1 lists the parameters used for the Eu^{3+} ion and each ligating atom (atom type, partial charge, and nonbonded parameters (r_{min} is the van der Waals radius, and e_{min} is the well depth potential)). Ligand molecules are entered as their fully deprotonated forms (in this case as −2 anions). The europium ions are entered as separate molecular entities each having a +3 charge. Eu^{3+} ions and ligands were brought into close proximity before minimization. Where necessary, manual adjustments were made to the ligand molecules to achieve the lowest possible energy after minimization. Energy minimizations were first carried out in vacuo, followed by reminimization inside a 30 Å sphere of solvent waters (TIP3P). No appreciable difference between the in vacuo and solvated complex structures was observed.

Results and Discussion

Ligand Design. Dpa is a well-studied lanthanide chelator.[29−31,54] It forms a 3/1 L/M complex with lanthanides in a classic three-bladed propeller arrangement (D_3 symmetry).[30] Since this structure is helical in nature (Λ or Δ chirality), it was decided to use $[Ln(dpa)_3]^{3-}$ (tris-dpa) as the basic building block for the construction of triple helical complexes which would be water soluble. Two dpa moieties are linked by various diamines, according to Scheme 1. The present work concerns the formation of helicates based on the achiral dpm and the chiral chxn spacers (Scheme 1).

Molecular Modeling of Helicates. Molecular mechanics calculations have been successfully used in the past to model the structures of lanthanide chelates in solution,[36,55,56] and such calculations are used as a guide in ligand design and to test the feasibility of various helical structures. It was possible to model

(53) Fritz, J. S.; Oliver, R. T.; Pietrzyk, D. J. *Anal. Chem.* **1958**, *30*, 1111−1114.
(54) Horrocks, W. D., Jr.; Sudnick, D. R. *Science* **1979**, *206*, 1194−1196.
(55) Wu, S. L.; Horrocks, W. D., Jr. *Inorg. Chem.* **1995**, *34*, 3724−3732.
(56) Wang, Y.; Horrocks, W. D., Jr. *Inorg. Chim. Acta* **1997**, *263*, 309−314.

Table 2. Structural Parameters of Helicate Models

ligand	structure	M−M Distance (Å)	av M−L distance (Å)	av pitch of dpa (deg)	total energy (kcal/mol)
dpa	crystal[a]	NA	2.49 (C)[c] 2.58 (P)	52	
	NMR[b]	NA	NR (C) 2.51 (P)	41	
	model	NA	2.37 (C) 2.60 (P)	40.5	
dpa-mma	model	NA	2.33 (C) 2.58 (P) 2.46 (A)	46.5	
dpa-chxn	helicate	8.0	2.33 (C) 2.59 (P) 2.46 (A)	38.2	−1831 (ΔΔ) −1813 (ΛΛ)
	meso-helicate	same as helicate	same as helicate	same as helicate	−1781
	linked	9.9	2.39 (wr C)/2.44 (brC) 2.60 (wr P)/2.59 (brP) 2.48 (wr A)/2.43 (brA)	46.2/73.8 41.8(br)	−1781
dpa-dpm	helicate	13.95	2.34 (C) 2.59 (P) 2.52 (A)	41	−1851
	meso-helicate	13.97	2.33 (C) 2.57 (P) 2.50 (A)	42	−1845

[a] $[Nd(dpa)_3]^{3-}$, from ref 30. [b] Reference 31. [c] A = amide carbonyl, C = charged oxygen, P = pyridine nitrogen, wr = wrapped ligand, br = bridging ligand.

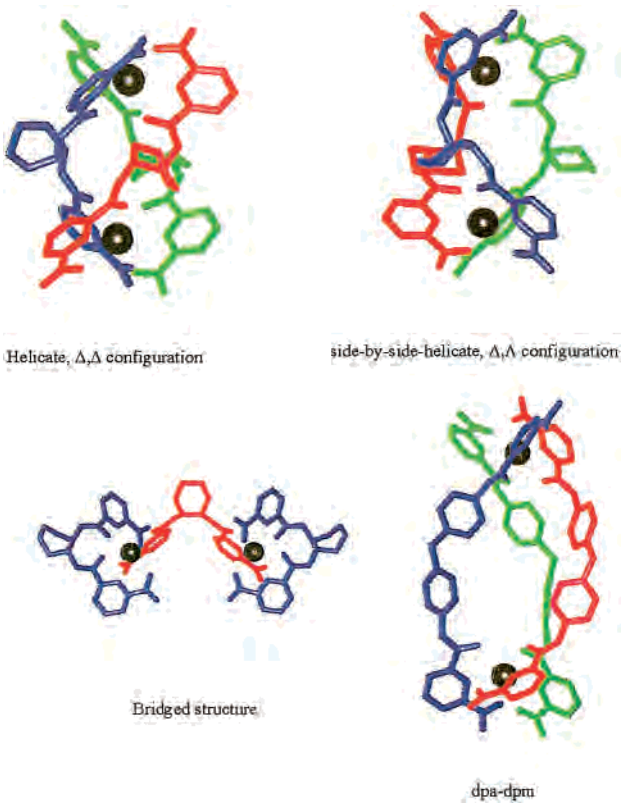

Figure 1. Possible structures for Eu^{3+} complexes of dpa-L ligands. Dpa-chxn-*S*,*S* is used as an example. The true helicate of dpa-dpm is also shown.

triple helical complexes for the two ligands studied here (Figure 1), both in true helix form (ΔΔ or ΛΛ configuration at the metal ion centers) and as side-by-side helicates (ΛΔ configuration (sbs helicates)). Dpa-chxn (but not dpa-dpm) also appears capable of forming a bridged structure, where one ligand wraps around so that both binding sites chelate one metal and the two wrapped metal ions are then bridged by the third ligand (Figure 1). The dpa-dpm ligand appears to be incapable of assuming a conformation necessary to have both of its binding sites coordinate to the same Ln^{3+} ion. Further, these modeled structures allow the determination of structural characteristics, such as metal−metal distance and hydrogen orientation, which are potentially useful in analyzing experimental luminescence energy transfer and NMR data on the complexes.

Table 2 lists some structural parameters determined from the modeling. Comparisons can be made between the modeled structures and the structure of tris-dpa determined from X-ray analysis and NMR.[30,57] Eu-ligating atom distances of the modeled tris-dpa are similar to those determined in both the X-ray and NMR structures of $[Eu(dpa)_3]^{3-}$, as is the pitch angle of the individual dpa ligands. The pitch angle is defined as the angle between the pseudo-C_3 axis and the plane of the dpa pyridine ring. The 0.12 Å difference in the M−O distance between the crystal structure and the model arises from the fact that the carboxylate groups are coplanar with the pyridine ring in the model structure, but are rotated out of the plane of the molecule in the crystal structure. In comparing the $[Ln(dpa)_3]^{3-}$ and $[Ln(dpa\text{-}mma)_3]$ structures, it appears that the distance between the Eu and the amide carbonyl (A) of dpa-mma has increased as compared to the Eu−O (C) distances in the dpa structures, which is expected owing to the greater affinity for the charged acidic oxygens by Ln^{3+} ions than for the neutral carbonyl oxygens of the amide group. This distance difference is also seen in the structures of the dinuclear complexes. The pitch angle of $Eu(dpa\text{-}mma)_3$ is larger than that for the dinuclear complexes, as is also the case for $[Eu(dpa)_3]^{3-}$. This may be due to constraints imposed by the spacer groups. On the basis of the structural parameters from molecular modeling, it appears that dpa-mma is a good model for the Ln^{3+}-binding sites of the dilanthanide complexes.

The bridged structure formed by dpa-chxn has a much more distorted binding site than the helical structures. The Ln−ligand distances listed in Table 2 are separated into those from the wrapped ligand (wr) and those from the bridging ligand (br). While the general trend of the Ln^{3+} ion being closer to the formally charged oxygen still holds, the binding site, when the angular distribution of ligating atoms is taken into account, is much more asymmetric than the distances indicate. The binding

(57) Reilley, C. N.; Good, B. W.; Desreux, J. F. *Anal. Chem.* **1975**, *47*, 2110.

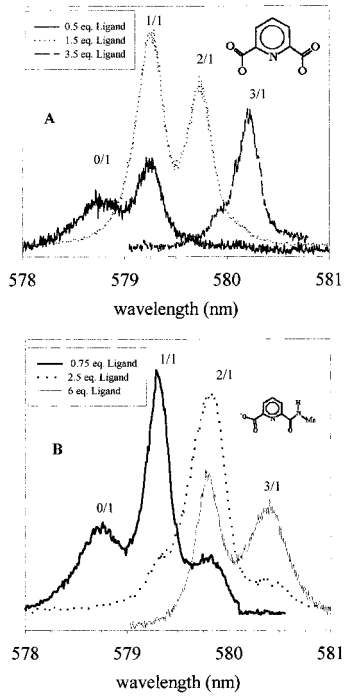

Figure 2. (A) A series of $^7F_0 \rightarrow {}^5D_0$ excitation spectra as dpa is added to 60 μM Eu^{3+}. (B) A series of $^7F_0 \rightarrow {}^5D_0$ excitation spectra as dpa-mma is added to 60 μM Eu^{3+} for 0.75 and 2.5 equiv spectra, and 10 μM Eu^{3+} for the 6.0 equiv spectrum.

site in the bridged structure has no real or effective 3-fold axis. The two tridentate binding units supplied by the wrapped ligand form an approximate equatorial plane, while the binding unit from the bridging ligand caps the coordination unit.

Energy calculations on the models for Eu_2(dpa-chxn-*R*,*R*)$_3$ indicate that the $\Delta\Delta$-helicate form is 18 kcal/mol lower in energy than its $\Lambda\Lambda$-diasteriomer (−1831 kcal/mol vs −1813 kcal/mol). Most of this energy difference is due to contributions from angular energy within the ligand molecules and electrostatics. The sbs-helicate and bridged models give essentially the same energy (−1781 kcal/mol), about 32 kcal/mol higher in energy than the $\Lambda\Lambda$-helicate. For comparison, molecular mechanics calculations on an achiral catechol-based Ga^{3+} helicate by Raymond et al.[58] indicates that its $\Lambda\Lambda$- and $\Delta\Delta$-helicates are 4.54 kcal/mol lower in energy than the corresponding *meso*-helicate.

One of the more useful parameters obtainable from molecular modeling is the metal−metal distance in the dilanthanide complexes. By forming complexes in the presence of a mixture of Eu^{3+} and Nd^{3+}, it is possible to determine metal−metal distances through energy-transfer measurements (vide infra).

Luminescence Spectroscopy of Eu^{3+}/Dpa complexes. The three-bladed propeller arrangement of ligands in $[Ln(dpa)_3]^{3-}$ forms the prototypical coordination site for the helicates.[30] Spectroscopic similarities between the trischelates and the helicates are to be expected. Figure 2A shows a series of $^7F_0 \rightarrow {}^5D_0$ Eu^{3+} excitation spectra as dpa is added to a solution of Eu^{3+} (60 μM Eu^{3+} in HEPES, pH 7). Peaks attributed to the 1/1, 2/1, and 3/1 L/M complexes are clearly evident. Table 3 lists the wavelengths, excited-state lifetimes, and number of coordinated water molecules determined for each complex. The crystal structure of $Eu(dpm)_3^{3-}$ shows no coordinated water molecules, and this is supported by the *q* value calculated from the luminescence data[30,54] for the species assigned to this species.

(58) Kersting, B.; Meyer, M.; Powers, R. E.; Raymond, K. N. *J. Am. Chem. Soc.* **1996**, *118*, 7221−7222.

Table 3. Excitation Peak Position, Luminescence Lifetime in H_2O and D_2O, Number of Coordinated Water Molecules, and Ligand/Metal Ratio for Dpa-Based Ligand/Eu^{3+} Complexes

ligand	peak wavelength (nm)	$\tau(H_2O)$ (μs)[a]	$\tau(D_2O)$ (μs)[a]	q (±0.1)	L/M ratio
dpa	578.72[b]	119	2791	9.0	0/1[b]
	579.25	164	2094	5.9	1/1
	579.73	335	2297	2.5	2/1
	580.36	1475	3113	0.1	3/1
dpa-mma	578.72	117	2740	8.8	0/1[b]
	579.32	177	2094	5.4	1/1
	579.79	393	2406	2.0	2/1
	580.45	1425	3150	0.1	3/1
dpa-dpm	578.72	118	2785	8.7	0/1[b]
	579.32	178	1872	5.3	1/2[c]
	579.94	619	2220	1.0	2/2[d]
	580.52	1478	2904	0.0	3/2
dpa-chxn	578.72	120	2737	8.5	0/1[b]
	579.40	210	2254	4.5	1/2[c]
	580.26	1564	3192	0.0	3/2
	580.70	1564	3192	0.0	3/2

[a] Error ±5% (ref 28 and references therein). [b] Eu^{3+}(aq). [c] Intermediate species found in very low concentrations possibly $[Eu_2L]^{4+}$. [d] Intermediate species found in very low concentrations possibly $[Eu_2L_2]^{2+}$.

Luminescence Spectroscopy of Eu^{3+}/Dpa-mma Complexes. As a control it was decided to make the "mononuclear" precursor of our triple helical complexes and to determine its luminescent properties. As shown in Scheme 1 one of the carboxylic acid groups of dpa is replaced with an amide group (methyl). Our intention was to determine what effect the amide group has on the binding to Eu^{3+} and the spectroscopy of the resulting complex, as dpa-mma is perhaps a better structural model for the binding site of the helicate-forming ligands than is dpa.

Figure 2B shows a series of luminescence excitation spectra as dpa-mma is added to Eu^{3+} (60 μM Eu^{3+} in HEPES, pH 7). Table 3 lists the wavelengths, luminescent lifetimes, and number of coordinated water molecules for the Eu^{3+}/dpa-mma complexes. The results are nearly identical to those for dpa with regard to peak wavelengths and measured lifetimes. The calculated numbers of coordinated water molecules also agree, within error.

Judging from the modeled dpa-based helicates and the Eu^{3+} luminescence spectra for $[Eu(dpa)_3]^{3-}$ and $Eu(dpa\text{-}mma)_3$ complexes, it is expected that the Eu^{3+} binding environment (in a fully formed helicate) will have no coordinated water molecules, an excitation peak in the vicinity of 580.35 nm, and an excited-state lifetime of about 1450 μs. Any intermediates which are formed prior to the complete assembly of the helical complex should show luminescence characteristics similar to those of the 1/1 and 2/1 L/M complexes of dpa-mma and dpa.

It should be noted here that our modeling predicts that two isomers of the 3/1 L/M complex should be formed, a *fac* complex (C_3 symmetry) and a *mer* complex (C_1 symmetry) existing statistically in a 1/3 ratio (25% *fac*, 75% *mer*). The molecular mechanics calculations show no significant difference in energy between these two isomers. There is no asymmetry in the 3/1 L/M peak (Figure 2B), which is broad and weak and could easily accommodate the presence of two isomers with similar first coordination spheres.

Luminescence Spectroscopy of Dpa-dpm. Figure 3 shows (A) representative spectra taken over the course of a titration of dpa-dpm into a 40 μM solution of Eu^{3+} as well as (B) a plot of the excitation intensities at various wavelengths vs the number of equivalents of ligand added during the titration. Table 3 gives

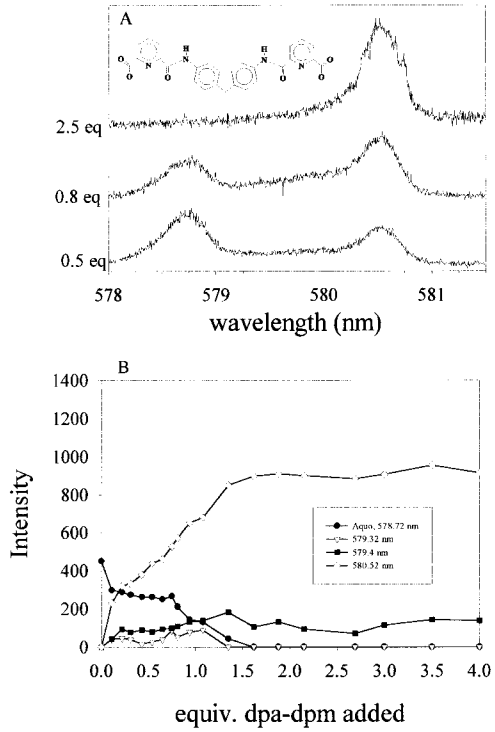

Figure 3. (A) A series of $^7F_0 \rightarrow {}^5D_0$ excitation spectra as dpa-dpm is added to 40 μM Eu^{3+}. (B) Peak intensity vs equivalents of dpa-dpm added to 40 μM Eu^{3+}.

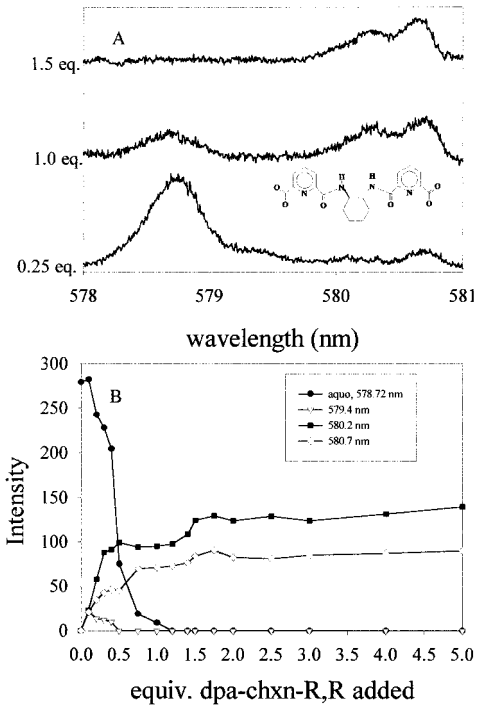

Figure 4. (A) A series of $^7F_0 \rightarrow {}^5D_0$ excitation spectra as dpa-chxn-*R,R* is added to 40 μM Eu^{3+}. (B) Peak intensity vs equivalents of dpa-chxn-*R,R* added to 40 μM Eu^{3+}.

the lifetimes and *q* values for each of the peaks observed during the course of the titration.

The most notable feature of the spectra shown in Figure 3 is that even in the early stages of the titration where free Eu^{3+} ion is still present (578.72 nm) the peak due to the final 3/2 L/M product (580.52 nm) is a prominent feature. This behavior is diagnostic of an apparently cooperative formation of the helicate species. The species responsible for the 580.52 nm peak has a 1510 μs lifetime, which leads to a *q* value of 0.35 water molecule (essentially 0 water molecules in the first coordination sphere). This peak position corresponds closely to that of $[Eu(dpa)_3]^{3-}$ (580.36 nm) and $[Eu(dpa\text{-}mma)_3]$ (580.45 nm), further indicating a helicate species. A plot of the intensities of this peak vs added equivalents plateaus beyond 1.5 equiv consistent with a complex of 3/2 L/M ratio. Other species are detectable in the course of the titration with signals that lie between those of the aqua ion and the helicate. While individual peaks are not easily resolvable and their intensities are low, lifetime spectroscopy indicates that these are likely 1/2 and 2/2 L/M species. Considering the fact that such lower-symmetry species generally are more highly luminescent than Eu^{3+}(aq) or tris complexes of D_3 symmetry, their concentrations are quite low at all metal/ligand ratios. The signal at 579.94 remains relatively constant beyond the break point in the titration and is likely a 2/2 species in equilibrium with the helicate, albeit a minor component of the system.

A titration of Tb^{3+} into a solution of the ligand yields the curve shown in the Supporting Information (Figure S1A). The excitation wavelength for this sensitized emission experiment is 350 nm, and the emission from the Tb^{3+} $^5D_4 \rightarrow {}^7F_5$ transition was recorded at 543 nm. The break point for this titration is at 0.67 equiv of added metal. This also establishes the 3/2 L/M stoichiometry of the complex.

Luminescence Spectroscopy of Dpa-chxn Ligands. Figure 4A shows some representative spectra taken over the course of a titration of dpa-chxn-*R,R* into a solution of 40 μM Eu^{3+}. Figure 4B shows a plot of the peak intensities vs number of equivalents of ligand added during the titration. Table 3 gives the lifetimes and *q* values for each of the peaks observed in the titration. The Supporting Information (Figure S1B) shows a titration of Tb^{3+} into a solution of dpa-chxn-*R,R* utilizing sensitized Tb^{3+} emission, with results similar to those of the titration done for dpa-dpm described above. Eu^{3+} and Tb^{3+} luminescence excitation and emission spectra are identical for dpa-chxn-*S,S* and dpa-chxn-*R,R*.

The Eu^{3+} excitation spectra have a number of notable features. First, there is an indication of an intermediate species formed (579.4 nm, $\tau = 210$ μs) but only at low added ligand concentrations (below 0.5 equiv of ligand). Second, the peaks at 580.70 and 580.26 nm, both with lifetimes of 1564 μs, appear at the earliest stages of the titration. These peaks are in the region of the spectrum, and possess a lifetime one would expect for a tris-dpa arrangement about europium. The *q* value (Table 3) is indicative of complete dehydration at the metal center. The fact that this complex is formed so early in the titration indicates that this is a highly favorable structure formed with apparent cooperativity. Third, at 1 equiv of ligand there is still a substantial signal from aqueous Eu^{3+}, indicating that most or all of the ligand present is going to form the tris-dpa-like helicate indicated by the 1564 μs lifetime and peaks at 580.25 and 580.7 nm. The plot of the peak intensities shows that the 1564 μs peak intensity levels off above 1.5 equiv of added ligand, at which point the weak signals from the intermediate complex and aqueous Eu^{3+} have vanished. The break point for this titration is consistent with the expected 3/2 L/M stoichiometry of the helical complex.

The other major feature of the luminescence spectroscopy of this system is that there are two peaks (580.2 and 580.7 nm), characteristic of the fully formed helicate. Measurement of the luminescence decays at the peak maxima yields the same lifetime value, 1564 μs. Both the 580.2 and the 580.7 nm peaks appear to be due to the same complex or isomers of a single complex, as is discussed further below.

Table 4. Metal−Metal Distances and Parameters Used for Calculation of Distance in Dpa-dpm and Dpa-chxn Complexes

parameter	dpa-dpm value (H_2O)	dpa-dpm value (D_2O)	dpa-chxn value (H_2O)
excitation λ (nm)	580.52	580.52	580.2/580.7
r, M−M dist (Å)	13.2	14.1	7.4
τ(Eu/Nd) (μs)	1256	2346	246
τ_0(Eu) (μs)	1478	2940	1564
E	0.150	0.192	0.843
ϕ	0.40	0.80	0.39
J (cm^6/mol)[a]	1.22×10^{-17}	1.22×10^{-17}	1.22×10^{-17}
R_0 (Å)	9.9	11.1	9.85

[a] Reference 36.

Metal−Metal Distances. Modeling studies of dpa-dpm and dpa-chxn give metal−metal distances, r, of 13.9 and 8.0 Å, respectively. $Eu^{3+} \rightarrow Nd^{3+}$ energy-transfer measurements of the distance between metal binding sites in dpa-dpm give a result of 13.7 ± 0.8 Å for the metal−metal distance, which is the average for the values determined from measurements in H_2O and D_2O. This is in good agreement with the model, and also clearly establishes the dinuclear nature of the complex. Parameters for the distance calculations are given in Table 4. $Eu^{3+} \rightarrow Nd^{3+}$ energy-transfer measurements of the distance between metal binding sites in the dpa-chxn-*R,R* helicate yield a distance of 7.4 ± 0.8 Å, close to the 8 Å distance expected for the helical species. Lifetime measurements obtained at both of the peaks yield the same result. Table 4 gives the parameters used in the calculation of the metal−metal distances. The modeled linked structure for dpa-chxn has a metal−metal distance of 9.9 Å (Table 2). There is no evidence that a complex with that metal−metal distance is formed. While modeling of the linked and helicate structures indicates that both should have similar luminescence properties, the energy-transfer result appears to rule out the linked structure.

Other Spectroscopy of Dpa-Based Helicates. To help determine the structure of the Ln^{3+}−ligand complexes, a number of studies were carried out using other spectroscopic techniques. Circular dichroism spectra of both bound and free dpa-chxn were recorded to see if it would be possible to establish the overall chirality of the helicate. A comparison of the emission spectra for Tb_2(dpa-dpm)$_3$ and Tb_2(dpa-chxn)$_3$ with D_3-symmetry $[Tb(dpa)_3]^{3-}$ and low-symmetry $Tb(dtpa)^{2-}$ (dtpa = diethylenetrinitrilopentaacetic acid) was also made to establish the overall symmetry of our helicates.

Studies on other helicate-forming ligands in nonaqueous solution[59,60] suggest that chiral ligands produce only one enantiomer of a helicate. The CD spectra of the free ligand dpa-chxn (both *R,R* and *S,S* enantiomers) clearly show it is chiral (Figure 5A). Also shown in Figure 5A is a spectrum in the 200−350 nm region of the ligand (dpa-chxn-*R,R*) complexed with Nd^{3+}. Ligand chirality is evident, although no Nd^{3+}-centered bands are seen in this wavelength range at a concentration of 10 μM. Figure 5B shows the CD spectrum of Nd_2(dpa-chxn-*R,R*)$_3$ in the 400−800 nm region where Nd^{3+} absorption bands lie. The CD spectrum clearly shows negative Cotton effects at about 583 and 720 nm, and a positive Cotton effect at 765 nm. The transition at 583 nm corresponds to the Nd^{3+} adsorption band $^4I_{9/2} \rightarrow {}^4G_{5/2}$, the 720 nm transition corresponds to the $^4I_{9/2} \rightarrow {}^4F_{7/2}$ band, and the 765 nm transition corresponds to the $^4I_{9/2} \rightarrow {}^2H_{9/2}$ Nd^{3+} band. This result indicates that the metal binding sites are chiral, and that both binding sites have the same chirality. The presence of both Δ and Λ configurations in the sbs-helicate would cancel the Nd^{3+}-centered Cotton effects.

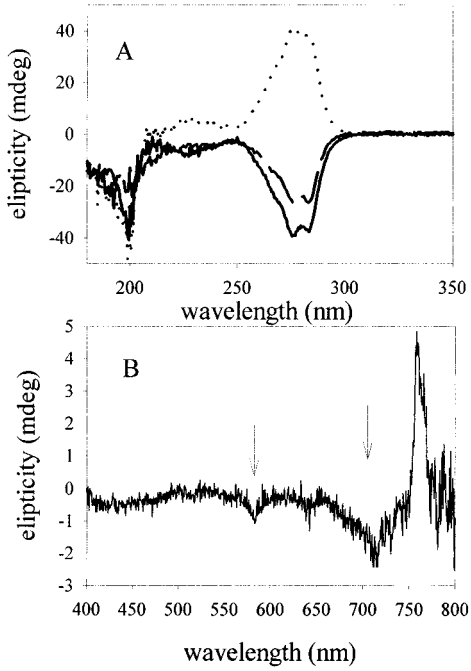

Figure 5. (A) Circular dichroism spectra of 30 μM uncomplexed dpa-chxn-*R,R* (solid line), 30 μM uncomplexed dpa-chxn-*S,S* (dotted line) and 10 μM Nd_2(dpa-chxn-*R,R*)$_3$ (broken line). (B) Circular dichroism spectra of 1 mM Nd_2(dpa-chxn-*R,R*)$_3$.

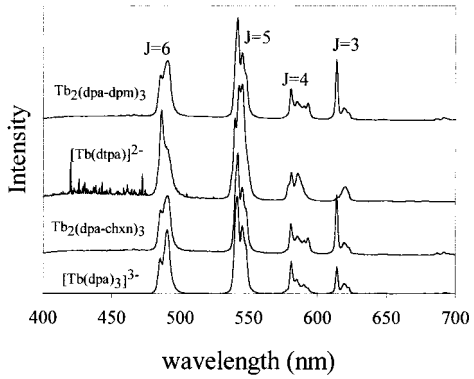

Figure 6. Comparison of Tb^{3+} emission spectra of Tb_2(dpa-chxn-*R,R*)$_3$ and Tb_2(dpa-dpm)$_3$ with those of Tb(tris-dpa) and Tb-dtpa.

The CD results do not establish the handedness ($\Delta\Delta$ or $\Lambda\Lambda$) at the metal centers. No solid-state CD has been reported on optically active crystals containing $Nd(dpa)_3^{3-}$ units (Na_3[Nd(dpa)$_3$] crystallizes in the centrosymmetric space group $P\bar{1}$ as a racemate[30]). The CD spectrum of an optically active crystal containing D_3 $Nd(oda)_3^{3+}$ (oda = oxydiacetate) is available,[61] but the authors failed to determine the handedness of the particular crystal used in their experiment.

Bünzli suggests that the luminescence emission profiles of the Tb^{3+} and Eu^{3+} complexes of his homodinuclear lanthanide helicates are characteristic of pseudo-D_3 complexes.[10,11] Figure 6 shows a comparison of the Tb^{3+} emission spectra of $[Tb(dpa)_3]^{3-}$, $[Tb(dtpa)]^{2-}$, Tb_2(dpa-dpm)$_3$, and Tb_2(dpa-chxn-*R,R*)$_3$. The Ln(III)/tris-dpa complex has been shown to have

(59) Zarges, W.; Hall, J.; Lehn, J.-M.; Bolm, C. *Helv. Chim. Acta* **1991**, *74*, 1843.
(60) Krämer, R.; Lehn, J.-M.; De Cian, A.; Fischer, J. *Angew. Chem., Int. Ed. Engl.* **1993**, *32*, 703−706.
(61) Vala, M.; Nath, D. N.; Chowdhury, M.; Wierzbicki, A.; Sen, A. C. *Chem. Phys. Lett.* **1987**, *134*, 610−616.

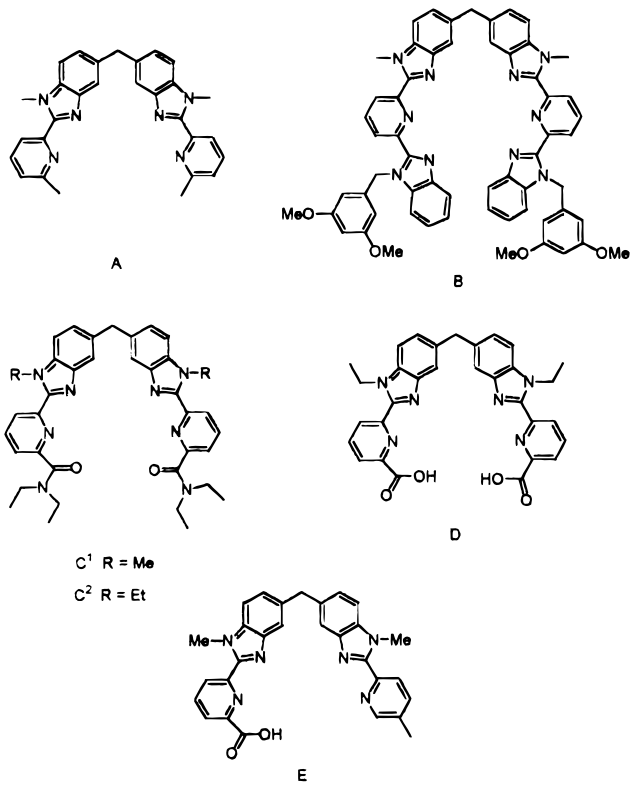

Figure 7. Triple helicate forming ligands which utilize the dpm linker (based on structures in refs 10−13).

D_3 symmetry.[30] The Ln-dtpa complex is of lower symmetry (as is typical of Ln(III) complexes with ligands of that type). The dpa-dpm- and dpa-chxn-based helicates are expected to have a D_3-like symmetry, and as expected, their emission spectra are quite similar to that of the tris-dpa complex and significantly different from that of the dtpa complex.

Comparison of Dpa-dpm Complexes with Other Helicates. The dpm spacer has been used by Bünzli et al.[10−12,14,19] (see Figure 7) for ligands which form helicates involving various metals (Co(II) and Ln(III)). Ligand A forms a triple helicate with Co(II), while ligands B, C^1, C^2, and D form homodinuclear triple helicates of Ln(III) ions. Ligand E forms a d−f triple helicate with Ln(III) and Zn(II). Helicates of A − D exhibit D_3 symmetry, while E yields complexes of C_3 symmetry. All the lanthanide helicates exhibit luminescence properties which can be compared to those of the present dpa-dpm complex. Ligands D and E are of particular interest because these binding sites have two ligating moieties in common with our ligands.

Eu^{3+} $^7F_0 \rightarrow {}^5D_0$ luminescence excitation spectra have not been reported for B−D-based helicates in solution, but have been recorded (at 77 and 295 K) on microcrystalline samples of B and $C^{1,2}$ (from acetonitrile solvent), which can be compared to our solution studies. Both complexes show bands for the $^5D_0 \rightarrow {}^7F_0$ transition in the range expected for a triple helicate based on a tris arrangement of metal binding sites (B, 580.5 nm (77, 295 K); C^1, 580.2, 580.8 nm (77 K), 580.2 (295 K); C^2, 580.5 nm (77 K)).[11] Helicates B−D all exhibit Eu^{3+} luminescence lifetimes consistent with no water molecules in the first coordination sphere of Eu, and show (by ^{1}H NMR) structures of D_3 symmetry in solution.

Luminescence excitation spectroscopy of Eu^{3+} in a heterodinuclear environment is reported for complexes of E in acetonitrile and H_2O solution, as well as for microcrystalline samples (from acetonitrile solution).[14] The $^7F_0 \rightarrow {}^5D_0$ excitation bands have maxima at 580.15, 580.35, and 580.21 nm for each of the samples, respectively. The excited-state lifetime recorded in aqueous solution indicates that there are no coordinated water molecules. The spectroscopic data for E are exactly in line with what we expect for a triple helical arrangement about Eu^{3+}. Eu(III) complexes of D should yield similar luminescence spectroscopy in solution, since its Ln(III) binding sites are the same as in E.

Identification of Peaks in the Luminescence Excitation Spectra of Eu_2(Dpa-chxn)$_3$. It still remains to identify what species are responsible for the two peaks seen in the $^7F_0 \rightarrow {}^5D_0$ excitation spectra of Eu_2(dpa-chxn)$_3$. The Eu^{3+} $^7F_0 \rightarrow {}^5D_0$ excitation band is between nondegenerate levels, so each peak observed in the spectra indicates a unique Eu^{3+} environment. A study of the $^5D_0$ excited-state lifetimes of Eu^{3+} for this complex indicates that each of these peaks has the same lifetime. Thus, it can be assumed that these two peaks arise from two binding environments which exclude waters to the same extent ($q = 0$), but which differ in some other (perhaps subtle) aspect of the Eu^{3+} first coordination sphere.

It was expected that a helicate with identical europium binding sites will give only a single peak in the excitation spectrum. A review of the literature shows that there are very few dinuclear lanthanide complexes (about eight different types, three of which are helicates) formed from either an individual chelator with multiple binding sites or multiple chelators (as in the case of the helicates).[10−12,36,62−65] The solution-state $^7F_0 \rightarrow {}^5D_0$ luminescence excitation spectra of four of these complexes (all nonhelicates) have been reported.[36,62,64] All of these show only a single peak in the $^7F_0 \rightarrow {}^5D_0$ excitation spectrum and, expectedly, exhibit only single-exponential excited-state decays.

The remaining spectra were recorded on microcrystalline samples (including two of the helicates).[10,11,62,63] The nonhelicates based on calix[8]arene[62,65] show essentially single transitions and single lifetimes for the dinuclear complexes. A Schiff base complex[63] exhibits two transitions, attributed to the presence of two slightly different metal binding sites in the molecule. The helicates also show spectra with multiple peaks which arise from two crystal forms, one highly symmetrical and one where a water molecule has associated with the helicate and lowered the symmetry of the molecule ($D_3 \rightarrow C_3$).[10,11] This analysis is supported by studies on the monomeric models of the binding sites for these helicates.[26,66] One helicate[11] also shows an additional transition in its spectra presumably from a slight asymmetry in the structure of the two binding sites.

Figure S2 in the Supporting Information shows the $^7F_0 \rightarrow {}^5D_0$ excitation spectra for dpa-chxn-*R*,*R* complexed with Eu^{3+} in acetonitrile, and a sample 1.6% v/v in water/acetonitrile solution. Only a single peak is observed in acetonitrile solution (580.3 nm), while two peaks are present in aqueous solution and in the mixed solvent system. This is an important clue as to the identity of the two peaks. As water is added to the acetonitrile solution, the single peak splits into two, with roughly the same splitting (580.6 and 580.2 nm) and same relative peak intensities as seen in 100% aqueous solution. This result is consistent with what is observed for two of Bünzli's helicates (above).[10,11] One of the peaks observed for dpa-chxn (580.26

(62) Bünzli, J.-C. G.; Froidevaux, P.; Harrowfield, M. *Inorg. Chem.* **1993**, *32*, 3306.
(63) Guerriero, P.; Vigato, P. A.; Bunzli, J.-C. G.; Moret, E. *J. Chem. Soc., Dalton Trans.* **1990**, 647.
(64) Ziessel, R.; Maestri, M.; Prodi, L.; Balzani, V.; Van Dorsselar, A. *Inorg. Chem.* **1993**, *32*, 1237.
(65) Bünzli, J.-C. G.; Ihringer, F. *Inorg. Chim. Acta* **1996**, *246*, 195.
(66) Renaud, F.; Piguet, C.; Bernardinelli, G.; Bünzli, J.-C. G.; Hopfgartner, G. *Chem. Eur. J.* **1997**, *3*, 1646.

nm) represents a helicate which somehow associates with a water molecule is such a way as to lower the symmetry of the helicate from D_3 to C_3. The other peak (580.75 nm) represents the more symmetric normal helicate. The association of the water molecule is not enough to affect the excited-state lifetime of Eu^{3+}, but the minor structural change is enough to show up in highly sensitive $^7F_0 \rightarrow {}^5D_0$ excitation spectra.

Determination of Conditional Stability Constants. The Horrocks laboratory has recently developed a direct luminescence spectroscopic method to determine the stability constant for Eu^{3+} complexes on the basis of competition between ligands.[37] A ligand (L′) with a known stability constant for its Eu^{3+} complex competes against a ligand (L) with an unknown stability constant for its Eu^{3+} complex for a limited amount of Eu^{3+}. The intensity of the Eu^{3+} $^7F_0 \rightarrow {}^5D_0$ transition for each complex is monitored, yielding a measure of the concentration of each species present. These data lead to the determination of the equilibrium constant for the competition reaction, K_{comp}:

$$Eu_2L_3 + 2L' \leftrightarrows 2EuL' + 3L \quad (6)$$

$$K_{comp} = [EuL']^2[L]^3/[Eu_2L_3][L']^2 \quad (M^2) \quad (7)$$

The thermodynamic formation constant, K_H, for the helicate-forming reaction

$$2Eu^{3+} + 3L \leftrightarrows Eu_2L_3 \quad (8)$$

is given by

$$K_H = [Eu_2L_3]/[Eu^{3+}]^2[L]^3 \quad (M^{-4}) \quad (9)$$

while the formation constant for the reference ligand L′, $K_{L'}$, is given by

$$Eu^{3+} + L' \leftrightarrows EuL' \quad (10)$$

$$K_{L'} = [EuL']/[Eu^{3+}][L'] \quad (M^{-1}) \quad (11)$$

K_H is thus given by

$$K_H = (K_{L'})^2/K_{comp} \quad (12)$$

A mixed ligand species is not accounted for in this analysis because there is no spectroscopic evidence that a mixed ligand complex is being formed. Wavelength scans and lifetime data show only Eu_2L_3 or Eu(nota) species.

It is important to take into account the fact that one or both ligands may be partially protonated under the experimental conditions. The conditional stability constants were therefore determined for the competition reactions (eq 6), $K_{cond,comp}$. In terms of $K_{cond,comp}$ and the tabulated thermodynamic constant, $K_{L'}$, for the reference ligand nota (nota = 1,4,7-triazacyclononane-*N*,*N*′,*N*″-triacetate), the thermodynamic constant for the helicate forming reaction (eq 8) is given by

$$K_H = ((K_{L'})^2/K_{cond,comp})(\alpha_{L'}{}^2/\alpha_L{}^3) \quad (13)$$

where α_L relates the stepwise protonation constants (K_1^H, K_2^H, etc.) of the ligand, L, and pH of the experiment:

$$\alpha_L = (1 + K_1{}^H[H^+] + K_1{}^HK_2{}^H[H^+]^2 + ...)^{-1} \quad (14)$$

Stability constants were determined for dpa-dpm and dpa-chxn utilizing nota as the competing ligand. In a typical experiment a 20 μM solution of helicate was formed (40 μM Eu^{3+}, 60 μM ligand) in pH 7 buffer (50 mM HEPES) and allowed to equilibrate for 24 h at 40 °C. Nota (50 μM) was added and the resulting mixture allowed to equilibrate for 24 h at 40 °C. The equilibrium concentrations of EuL′ and Eu_2L_3 were determined from the calibrated intensities (peak maximum for each complex) of the $^7F_0 \rightarrow {}^5D_0$ excitation spectra (at 25 °C), and the equilibrium concentrations [L′] and [L] were calculated with knowledge of initial concentrations of Eu^{3+}, L, and L′, assuming there to be no free Eu^{3+} present.

Table S1 lists the concentrations of species determined in the experiment. The stability constant for the Eu(nota) system is $\log K_{L'} = 13.7$ (K in units of M^{-1}) (with protonation constants of $\log K_1^H = 11.4$, $\log K_2^H = 5.74$, $\log K_3^H = 3.16$, and $\alpha = 3.8 \times 10^{-5}$ at pH 7).[67] The thermodynamic stability constants for the two helicate ligands are essentially the same, $\log K_H = 31.6 \pm 0.2$ (K_H in units of M^{-4}). Protonation constants for the dpa-based ligands have not been determined but should be similar to those of dpa-based ligands ($\log K_1^H = 5.09$, $\log K_2^H = 2.25$, $\alpha = 0.988$ at pH 7).

For ligand D (Figure 7) stability constants in aqueous solution (determined from spectrophotometric titrations) were reported for several Ln(III) complexes.[12] The Eu(III) complex has a stability constant of $\log K = 26.1 \pm 0.4$. This result compares favorably to our findings. Differences between that value and ours can be attributed to (1) the use of estimated protonation constants for our ligands, (2) the presence of a less favorable nitrogen ligand in the binding site of the Bünzli helicate as compared to the carbonyl ligand in ours, and (3) the fact that no account was taken of the possible formation of a 2/2 L/M complex in the fit of their titration data. The stability constants in acetonitrile solution of the other Bünzli helicates are reported to be about $\log K = 21$ for ligand B and $\log K = 24.1$ for ligand C[1].[10,11] Both of these helicates are unstable in aqueous solution. Helicates based on E are stable in aqueous solution, but experimental difficulties did not allow for the determination of a stability constant for its helicate in either acetonitrile or water.[14]

Conclusions

Although definitive proof that the dpa-dpm and dpa-chxn ligands form triple helical complexes with Ln(III) ions can come only from an X-ray crystal structure of the complex, we believe we have sufficient evidence to conclude that these two ligands do indeed form triple helicates in the presence of Ln(III) ions. Comparison of the Eu^{3+} luminescence excitation spectra in aqueous solution of $Eu_2(dpa\text{-}dpm)_3$ and $Eu_2(dpa\text{-}chxn)_3$ with Eu^{3+} luminescence excitation spectra of four known Ln(III) triple helicates shows peak maxima in the same region, in two cases with identical wavelengths. Also the $^7F_0 \rightarrow {}^5D_0$ transitions of our two complexes closely resemble those observed in the excitation spectra of the $[Eu(dpa)_3]^{3-}$ and $[Eu(dpa\text{-}mma)_3]$ models for the binding site of the helicate. Eu^{3+} excited-state lifetimes also confirm the expected exclusion of all water molecules from the first coordination sphere of Eu^{3+} in the helicates. Tb^{3+} emission spectra further show that the dpa-dpm and dpa-chxn helicates have the expected D_3-like symmetry and establish the 3/2 L/M stoichiometries of $Tb_2(dpa\text{-}dpm)_3$ and $Tb_2(dpa\text{-}chxn)_3$. $Eu^{3+} \rightarrow Nd^{3+}$ energy transfer proves the dinuclear nature of both complexes, and the metal−metal distances of 13.7 ± 0.8 Å for $Ln_2(dpa\text{-}dpm)_3$, and 7.4 ± 0.8 Å for $Ln_2(dpa\text{-}chxn)_3$ obtained from these experiments compare well with the

(67) Brucher, E.; Cortes, S.; Chavez, F.; Sherry, A. D. *Inorg. Chem.* **1991**, *30*, 2092−2097.

metal−metal distances derived from molecular modeling of the helicates. Stability constants determined for our complexes also compare favorably with that determined for the water-soluble helicate of Bünzli.[12,13]

Studies of other helicate-forming systems indicate that chiral ligands form enantiomerically pure helicates, while achiral ligands form racemic mixtures of helicates. CD spectroscopy of the complexes formed by dpa-chxn-*R*,*R* with Nd^{3+} show Cotton effects for some of the Nd^{3+} absorption bands. This indicates that the metal binding sites of the complex are chiral (as expected for a helicate) and that both metal binding sites have the same chirality (as is expected for true helicates). Molecular mechanics calculations predict that the $\Delta\Delta$ conformation of Eu_2(dpa-chxn-*R*,*R*)$_3$ is more stable by about 18 kcal/mol than the $\Lambda\Lambda$ conformation.

Expansion of ligands of this type to form longer helical polynuclear structures is obvious. The trinuclear and higher homologues in the series will be charged, which should increase their solubility in water and, perhaps, allow them to interact with chiral and/or helical biomolecules such as DNA. Applications in the clinical assay and photonic device areas may be possible for such species in the future.

Acknowledgment. This work was supported by the National Science Foundation through Grant CHE-9705788. We thank Dr. S.-L. Wu, R. M. Supkowski, and M. E. Panek for helpful discussions and other assistance. We thank Dr. C. R. Matthews for the use of his CD spectrometer. We also thank Dr. T. E. Glass and Dr. X. M. Zhang for helpful advice in the synthesis of the ligands.

Supporting Information Available: Figures showing the titration of Tb^{3+} into 60 μM dpa-dpm and 60 μM dpa-chxn-*R*,*R* and comparison of the $^7F_0 \rightarrow {}^5D_0$ excitation spectra of Eu_2(dpa-chxn-*R*,*R*)$_3$ in pure acetonitrile and as water is added and a table giving the concentrations for calculations of conditional stability constants. This material is available free of charge via the Internet at http://pubs.acs.org.

IC990698L